Finite Element Simulation of Ultrasonic Waves in Corroded Reinforced Concrete for Early-stage Corrosion Detection

Qixiang Tang and Tzuyang Yu

Department of Civil and Environmental Engineering
University of Massachusetts Lowell
One University Avenue, Lowell, MA 01854, U.S.A.

ABSTRACT

In reinforced concrete (RC) structures, corrosion of steel rebar introduces internal stress at the interface between rebar and concrete, ultimately leading to debonding and separation between rebar and concrete. Effective early-stage detection of steel rebar corrosion can significantly reduce maintenance costs and enable early-stage repair. In this paper, ultrasonic detection of early-stage steel rebar corrosion inside concrete is numerically investigated using the finite element method (FEM). Commercial FEM software (ABAQUS) was used in all simulation cases. Steel rebar was simplified and modeled by a cylindrical structure. 1MHz ultrasonic elastic waves were generated at the interface between rebar and concrete. Two-dimensional plain strain element was adopted in all FE models. Formation of surface rust in rebar was modeled by changing material properties and expanding element size in order to simulate the rust interface between rebar and concrete and the presence of interfacial stress. Two types of surface rust (corroded regions) were considered. Time domain and frequency domain responses of displacement were studied. From our simulation result, two corrosion indicators, baseline (b) and center frequency (f_c) were proposed for detecting and quantifying corrosion.

Keywords: Finite element method (FEM), damage detection, rebar corrosion

1. INTRODUCTION

In the past, fiber optic sensors (FOS) have been successfully applied in civil engineering for monitoring strains, displacements, and cracks of reinforced concrete (RC) and steel structures,[1] as well as for nondestructive testing (NDT) and structural health monitoring (SHM) applications.[2] Taking advantage of the small size of FOS, civil engineers can measure internal status of RC structures without introducing significant effect of stress concentration, during and after construction.[3,4] An ultrasonic FOS prototype has been proposed to actively monitor the local condition inside RC structures by utilizing the surface wave generated by the FOS.[5,6] The active sensing capability of such FOS prototype can be applied to the early-stage detection of steel rebar corrosion inside RC structures. Nonetheless, surface wave propagation behavior inside RC structures need to be better studied.

The objective of this study is to better understand the surface wave propagation behavior of ultrasonic signals between steel rebar and concrete in RC structures. In this research, the wave propagation behavior of an ultrasonic wave with center frequency of 1 MHz was studied. Finite element (FE) method was applied in building numerical RC models and simulating wave propagation in RC models. A commercial FE software package ABAQUS® (by Dassault Systems) was chosen for its wide applications in explicit analysis. Two FOS were distributed on both sides of a rebar model, in order to efficiently detect surface corrosion between two FOS.[7] Time domain and frequency domain responses were analyzed for corrosion detection.

In this paper, FE modeling of intact and corroded rebar models is first described. Design of FE models and characterization of artificial corrosion are provided. Two corrosion indicators based on the time domain and frequency domain displacement responses are proposed for locating and quantifying surface corrosion. Finally, a corrosion detection method is proposed from research findings.

Further author information: (Send correspondence to T. Yu)
E-mail: tzuyang_yu@UML.EDU, Telephone: 1 978 934 2288

Table 1. Material properties

	Steel	Concrete	Rust
Density (kg/mm^3)	7.85×10^{-6}	2.24×10^{-6}	2.61×10^{-6}
Young's Modulus (MPa)	210×10^3	41×10^3	500
Poisson's ratio	0.3	0.2	0.3

2. FINITE ELEMENT MODELING

To study the surface wave propagation in intact and corroded RC structures, two dimensional (2D) FE models were designed and used. An intact model was created first with 78,744 linear plain strain elements. Geometry of the rebar was simplified as a rod. By introducing artificial corrosion to the intact model, two different corroded models were made. Displacement responses were collected and analyzed.

2.1 Intact Model

The intact model (IM) was designed based on a steel rod with 12.7 mm (0.5 in) diameter, embedded in a 200mm-by-200mm concrete block, as shown in Fig. 1. A FOS transducer and a FOS receiver were distributed on the rebar model. Detailed features of a rebar such as ribs and lugs of the rebar were not included in this research. The properties of steel and concrete are provided in Table 1.
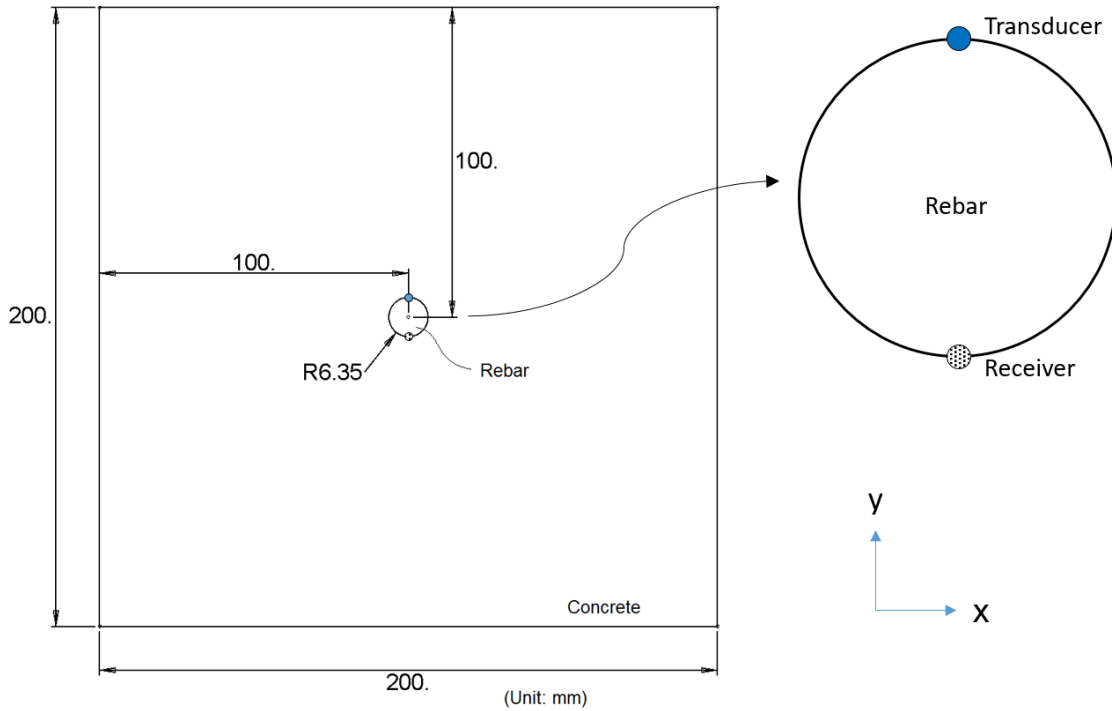

Figure 1. Simplified 2D RC model

All edges of the intact model were free, and the interaction between rebar and concrete was assumed to be perfectly bonded, as shown in Fig. 2. 2D plain strain element (CPE4) were used in the intact model. Bias meshing was applied in order to reduce the number of elements.

The FOS transducer, generated a sinusoidal pulse (Fig. 3). The FOS receiver collected time domain displacement response in the y- direction $u(t)$ (shown in Fig. 4).
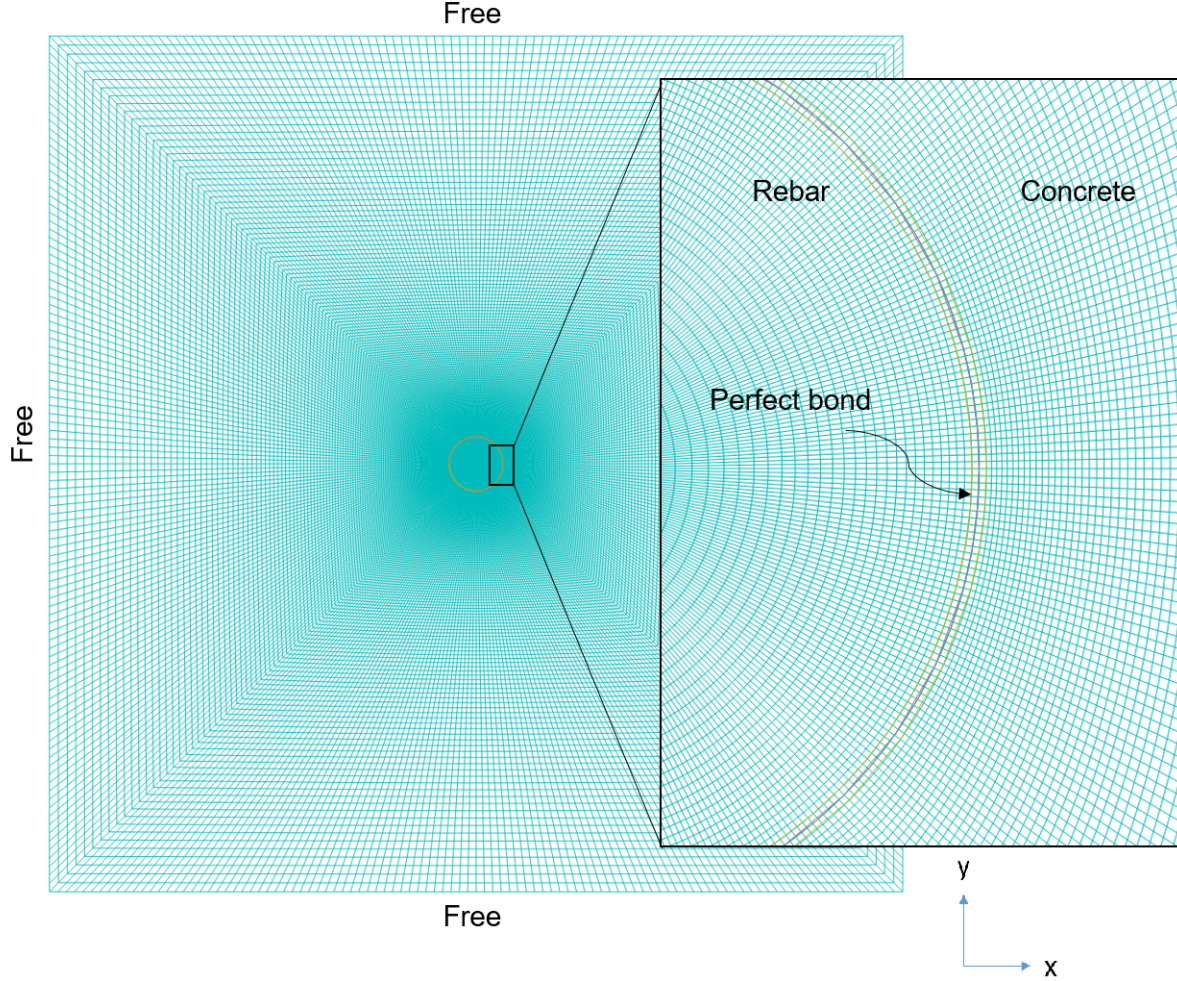
2

Figure 2. Meshing of the intact model

2.2 Corroded Models

Two corroded models, global corrosion model (GCM) and local corrosion model (LCM), were created by introducing artificial corrosion to the intact model. Two types of artificial corrosion were used in this research; global corrosion and local corrosion, as shown in Fig. 4.

- Global corrosion – As shown in Fig. 4, global corrosion was a rust layer surrounding the rebar with a thickness (h) of 0.1mm. The outer diameter of the rust layer was 12.7 mm (0.5 in). The arc length (a) (or perimeter) of global corrosion was 39.897mm.

- Local corrosion – A local corrosion was a section of global rust layer, as is shown in Fig. 4. The arc length (a) of this section was 3.32 mm (0.13 in).

Two realistic corrosion processes were considered; 1) generation of internal stress due to volumetric expansion of corrosion; 2) material property changes from steel to rust. These two processes were carried out by using the following.

1. Defined the material properties in corroded region to be temperature dependent.[8] The material properties (e.g. density, Young's modulus and Poisson's ratio) was steel when temperature (T) was 0 K, which was set
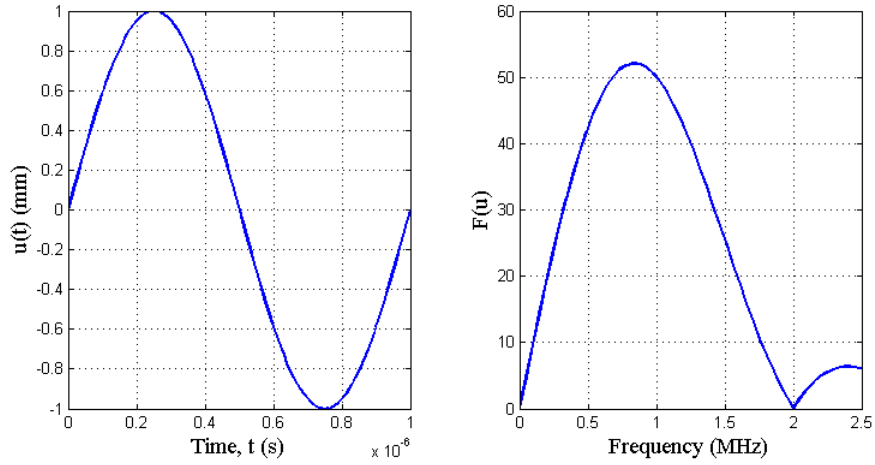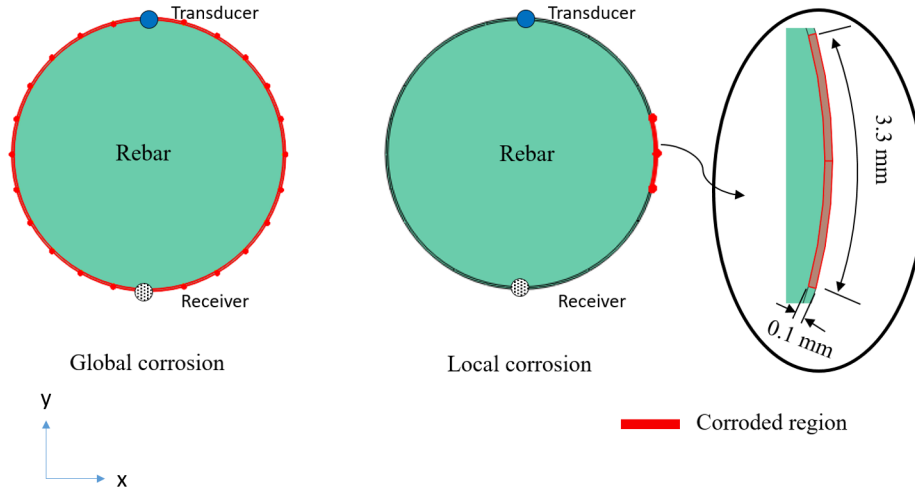
3

Figure 3. Loading function

Figure 4. Configuration of FOS transducer and receiver and corrosion types

as the default temperature. When temperature became 1 K, material changed from steel to rust, as shown in Table 1. Material at un-corroded region were independent from temperature, and thermal transfer was not included in these models.

2. Defined the thermal expansion coefficient α, which indicated the change in a material's area due to a change in temperature, as 2 K^{-1}. The area of corrosion region expanded for two times when temperature increased for 1 K.

3. Increased the temperature in corroded region from 0 K to 1 K. As a result, internal stress was created by the expansion of corroded region, and the material was updated from steel to rust.

After introducing artificial corrosion to the model, ultrasonic waves were generated at the transducer. These waves propagated in the FE model and caused time domain displacement responses. The receiver, as shown in Fig. 4, collects time domain displacement responses in y- directions (u(t)).

4

Since expansion of corrosion would cause internal stress/strain at the receiver's location, it resulted in a constant time domain displacement response. This constant displacement response became a baseline (b) of u(t). Eq.(1) was used to calculate the baseline (b) of $u(t)$.

$$b = \left| \frac{\Sigma_{t=t_0}^{t=t_n} u(t)}{n} \right| \tag{1}$$

where b = baseline (mm), u(t) = time domain displacement response (mm), t = time (s) and n = number of data points in u(t).

3. SIMULATION RESULTS

3.1 Time Domain Displacement Responses

Time domain displacement responses u(t) was collected by the receiver from intact and corroded models, as shown in Fig. 5. Baselines were found in time domain displacement of two corrosion models. The baseline of each corrosion model was calculated by Eq.(1) and listed in the Table. 2. It was found that, when corrosion size increased from LCM to GCM, baseline became greater. The baseline of GCM was 258.13 times greater than the one of LCM.

Baselines were removed by subtracting them from time domain displacement response u(t) of corroded models and shown in Fig. 6. The time domain displacement response of LCM and IM were similar to each other, comparing with the one of GCM was different from them.

In terms of amplitude (of u(t)), for example, the peak value of three models were: IM – 3.02×10^{-3} mm; LCM – 3.25×10^{-3} mm (7.62% of difference from IM); GCM – 3.6×10^{-3} mm (20.53% of difference from IM).

In terms of phase shift, LCM had much less effect than GCM. As an example, arrival time of each peak value were: IM – 7.40×10^{-6} mm; LCM – 7.41×10^{-6} mm; GCM – 10.60×10^{-6} mm. The differences in arrival time caused by local and global corrosion were 0.14% and 43.24%.
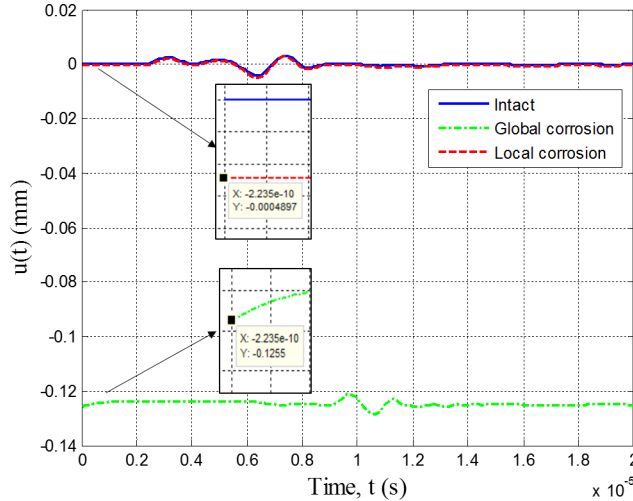

Figure 5. Time domain displacement response

5

Table 2. Baseline of each model

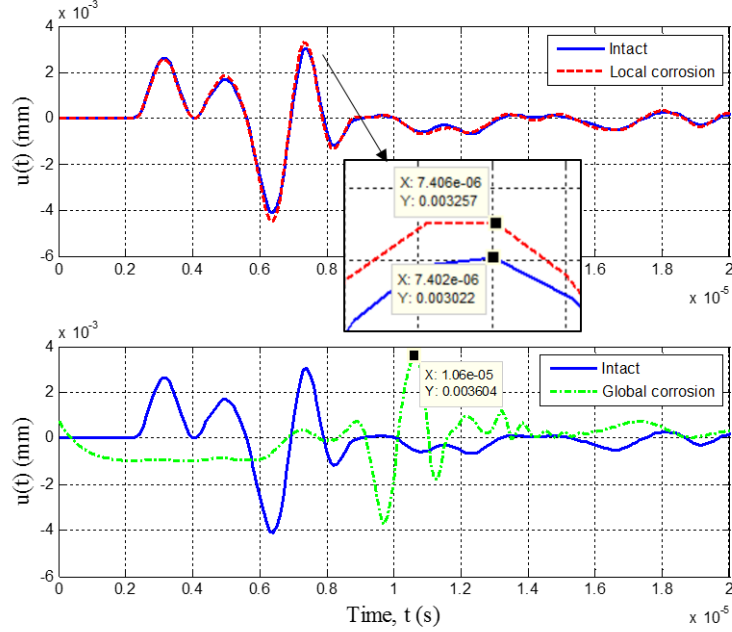|	Baseline (b) (mm)
Intact model (IM)	0
Local corrosion model(LCM)	4.8425×10^{-4}
Global corrosion model (GCM)	0.125

Figure 6. Time domain displacement response without baseline

3.2 Frequency Domain Response

By conducting fast Fourier transform (FFT), time domain displacement responses were converted into frequency domain. Frequency responses of FE models were shown in Figs. 7 to 9. Note that the frequency of any baseline was 0 Hz since it was a constant. Greater baseline leaded to greater amplitude of 0 Hz component. As an example, frequency domain response of GCM had greatest 0 Hz component among three models.

Gaussian curve fitting was applied to frequency domain reposes, as shown in Figs. 7 to 9. Center frequency (f_c) of each frequency domain response was found from the corresponding fitted curve in its frequency spectrum and listed in Table 3. It was found that when corrosion size increases, center frequency decreases.

3.3 Corrosion Indicators

- Baselines (b) – Because the baseline represened a constant displacement at receiver caused by corrosion, it was select as an indicator for corrosion detection. For example, in the intact model, the baseline was zero. By introducing a local corrosion, baseline value increases to 4.8425×10^{-4} mm. It was found that, when corrosion size (arc length(a)) increased, baseline also increased. This relationship was described by Eq. (2).

$$a = 1.657 \exp{(25.45b)} \tag{2}$$

Table 3. Center frequencies

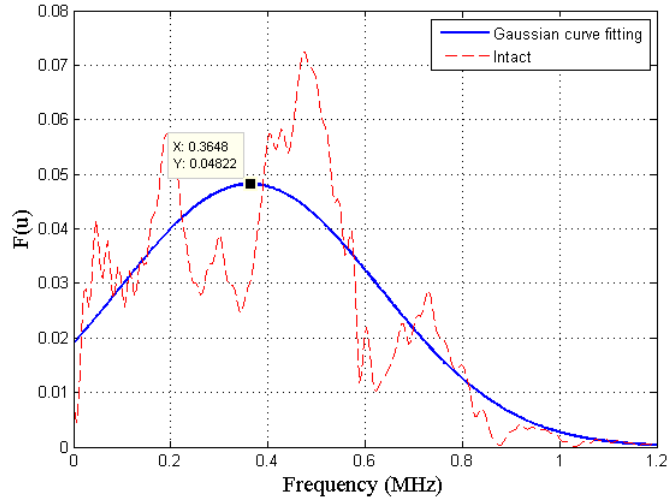|	Arc length (mm) (a)	Center frequency (f_c) (MHz)
Intact model (IM)	0	0.365
Local corrosion model (LCM)	3.32	0.159
Global corrosion model (GCM)	39.897	0

6

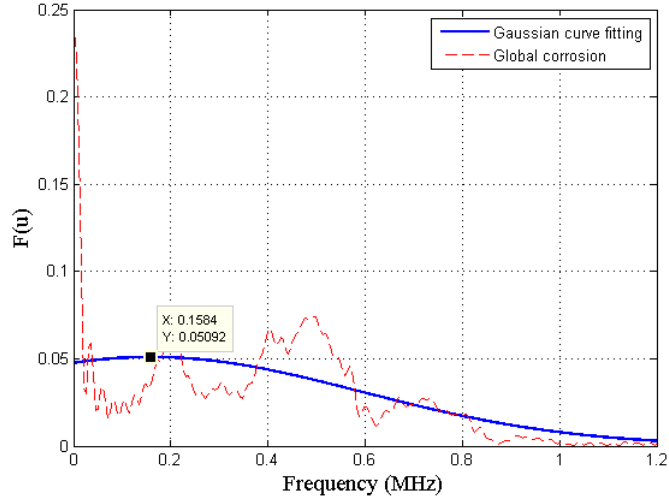Figure 7. Frequency response of intact model

Figure 8. Frequency response of local corrosion model

where $a=$ arc length of corrosion (mm) and $b =$ baseline (mm).

- Center frequency (f_c) – As shown in Table 3, the value of center frequency reduced when arc length (of corrosion) increased. As an example, arc length in the intact model is zero. By introducing a local corrosion, center frequency f_c decreased from 0.365 MHz to 0.159 MHz. This relationship between f_c and arc length (a) was described by Eq. (3).

$$a = 39.9 \exp\left(-15.38 f_c\right) \tag{3}$$

where $a=$ arc length of corrosion (mm) and $f_c=$ center frequency (MHz).

4. CONCLUSION

This paper reports our 2D numerical investigation on the surface corrosion detection using surface ultrasonic waves. Major research findings are summarized in the following.
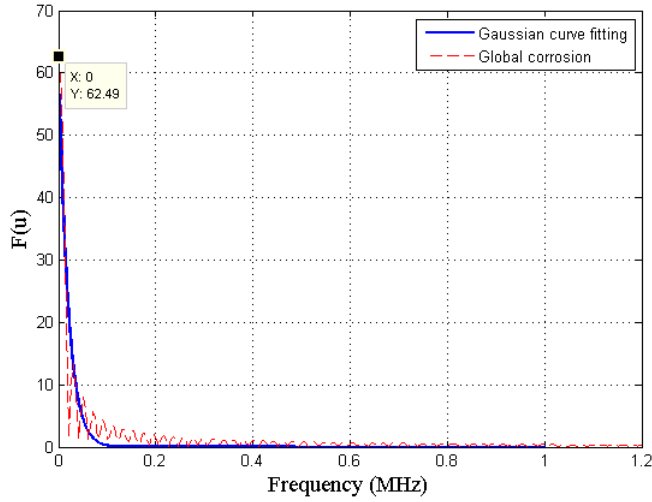
7

Figure 9. Frequency response of global corrosion model

- The presence of corrosion at the interface between steel rebar and concrete can be detected by the change of radial displacement (($u(t)$) in this research). The appearance of corrosion results in the decrease of time domain displacement response $u(t)$ in a transmission sensing scenario. This decrease is a constant value and is defined as the baseline (b). Non-zero values of b suggest the appearance of corrosion. In this study, non-zero baselines were found from both local and global corrosion models (Fig. 5).

- In the time domain, when the size of corrosion (arc length (a)) grows, the baseline (b) in radial displacement also increases. For example, baseline of GCM is 258.13 times greater than the one of LCM. The empirical equation (Eq. (2)) is proposed to estimate the corrosion size.

- In the frequency domain, when the size of corrosion (arc length (a)) increases, center frequency f_c of radial displacement decreases. For example, center frequency f_c decreases from 0.365 MHz to 0.159 MHz when a local corrosion is introduced to the intact RC model. This relationship can be described by Eq. (3).

- A corrosion detection method is proposed here; 1) Measure time domain displacement response in radial direction ($u(t)$); 2) Calculate baseline b from the obtained time domain displacement response using Eq. (1); 3) If the baseline is not zero, it indicates the existence of corrosion; 4) Once the corrosion is detected, corrosion size can be estimated using predetermined relationship (i.e., Eq.(2)) between arc length (a) and baselines(b). Alternatively, center frequency (f_c) can also be used to estimate corrosion size with following steps; 1) Measure time domain displacement response in radial direction ($u(t)$) and converted it to the frequency domain; 2) Apply Gaussian curve fitting to the frequency spectrum and find the center frequency (f_c). 3) Use predetermined relationship (i.e., Eq.(3)) between arc length (a) and center frequency (f_c) to estimate corrosion size. However, frequency responses always contain noises in practice. Therefore, Eq.(3) needs to be used with caution.

In this paper, two corrosion indicators, baseline (b) and center frequency (f_c), are proposed for detecting and quantifying corrosion. A corrosion detection method utilizing baseline (b) and center frequency (f_c) is summarized. This method can be used as guidance for inspecting and monitoring corroded RC structures with small sensors (e.g., FOS).

5. ACKNOWNLEDGEMENT

REFERENCES

[1] Ansari, F., "Structural health monitoring with fiber optic sensors," Frontiers of Mechanical Engineering in China , 169–196 (2009).

[2] Mendez, A. and Graver, T., "Overview of fiber optic sensors for ndt applications," Proceedings of IV NDT Panamerican Conference (2007).

[3] Zou, X., Chao, A., Tian, Y., Wu, N., Zhang, H., Yu, T., and Wang, X., "An experimental study on the concrete hydration process using fabryperot fiber optic temperature sensors," Measurement 45 (2012).

[4] Zou, X., Chao, A., Tian, Y., Wu, N., , Yu, T., and Wang, X., "A novel fabry-perot fiber optic temperature sensor for early age hydration heat study in portland cement concrete," Smart Structures and System 12 (2013).

[5] Zou, X., Schmitt, T., Perloff, D., Wu, N., Yu, T., and Wang, X., "Nondestructive corrosion detection using fiber optic photoacoustic ultrasound generator," Measurement 62, 74–80 (2015).

[6] Wu, N., Zou, X., Zhou, J., and Wang, X., "Fiber optic ultrasound transmitters and their applications," Measurement 79, 164–171 (2016).

[7] Tang, Q. and Yu, T., "Finite element simulation for damage detection of surface rust in steel rebars using elastic waves," Proceedings of SPIE Vol. 9804 (2016).

[8] Dassault Systémes, 10 rue Marcel Dassault, CS 40501, 78946 Vélizy-Villacoublay Cedex-France, Abaqus/CAE User's Manual Version 6.12.

[9] Zou, X., Schmitt, T., Perloff, D., Wu, N., Yu, T., and Wang, X., "Nondestructive corrosion detection using fiber optic photoacoustic ultrasound generator," Measurement 62, 74–80 (2015).